Scaling Exponent and Kuhn Length of Pinned Polymers by Single Molecule Force Spectroscopy

Ferdinand Kühner, Matthias Erdmann, and Hermann E. Gaub

Chair for Applied Physics and Center for NanoScience, Ludwig-Maximilians Universität München, Munich, Germany
(Received 7 April 2006; published 20 November 2006)

The end-to-end distance and the contour length of single polymers in dynamic adsorbate layers were measured with a mechanical approach. Individual polysaccharide chains were covalently pinned to the surface with one segment and picked up randomly with an atomic force microscope tip. The polymer section between pinpoint and the pickup point was stretched by retracting the tip from the surface. The pinpoint was derived by measuring the normal force while laterally scanning the surface at constant height. For carboxy-methyl-amylose, a Kuhn length of 0.44 nm and a scaling exponent of 0.74 were found.

Both conformation and dynamics of polymers govern their function in numerous applications, e.g., as coatings, adhesives, in composite materials, or the like. A rich body of literature on both theory [1–4] and modeling exists [5,6], and a wealth of experimental data is available [7]. Ensemble measurements, such as light scattering [8,9], have in many instances corroborated theoretical predictions on the scaling of the end-to-end distance of a polymer $\langle|R|\rangle$ and N, the number of segments which follows $\langle|R|\rangle \approx bN^\nu$. Here b is the Kuhn length and ν the critical exponent, which depends on the dimension of the system and has a value of $\nu = 1$, 0.75, 0.588, and 0.5, for $d = 1$, 2, 3, and $d \geq 4$, respectively [1]. If one expresses the number of units N by the contour length $L_c = bN$, both the end-to-end distance $\langle|R|\rangle$ and L_c are linked by the simple relation $\langle|R|\rangle \approx L_c^\nu b^{(1-\nu)}$. A double logarithmic plot of the end-to-end distance $\langle|R|\rangle$ against L_c should thus result in a linear dependency and provide ν.

Since ensemble experiments average over a large population of polymers, individual details of the polymer molecules remain hidden, and, in polydisperse samples, length-dependent deviations are concealed. Single molecule experiments overcome such obstacles. Conformational transitions (dextran [10], titin [11], or DNA) and solvent-mediated supramolecular rearrangements were discovered [12,13], and new models for the polymer elasticity based on an interplay between backbone deformations and entropic conformations were developed [14–16].

For polymers at surfaces, scanning probe techniques were employed *in situ* and on dried samples [17–22]. However, under conditions where the lateral mobility of the polymers exceeds the cantilever scanning speed, no high-resolution imaging is possible. Recently, we and others discovered that weakly adsorbed polymers might exhibit an unexpectedly high in-plane mobility [23], although their adhesion enthalpy per segment exceeds several $k_B T$ resulting in a quasi-irreversible adsorption already at short polymer lengths [24–26]. Because of the high in-plane mobility, information on the conformation of the polymers could not be gained up to date, even though

such adsorbate layers are ideal model systems for polymer solutions with reduced dimensionality. In this Letter, we develop a strategy to derive the key parameters for the conformation, the Kuhn length b and the scaling exponent ν, by measuring the contour length and the end-to-end distance of individual polymers. The experimental strategy is outlined in Fig. 1.

Carboxy-methyl-amylose (CMA) was covalently pinned to a glass slide [27,28] with such a low efficiency that the probability to pick up a polymer with the atomic force microscope (AFM) tip was less than 1%. The lateral density was confirmed by AFM imaging to be 12 molecules per μm^2 (see supplementary material [29]). This low surface density of attachment sites also ensures that the vast majority of the polymers are bound to the surface only at one segment.

Pinning at one point just restricts the large-scale mobility but leaves the conformational freedom of the polymer in 2D unaltered. Since the amino functionalized glass surface is positively charged, the weakly negatively charged CMA polymer is expected to absorb to the surface. We confirmed this in single molecule desorption measurements (see supplementary material [29]) where we found long force plateaus between 8–9 pN. This value converts
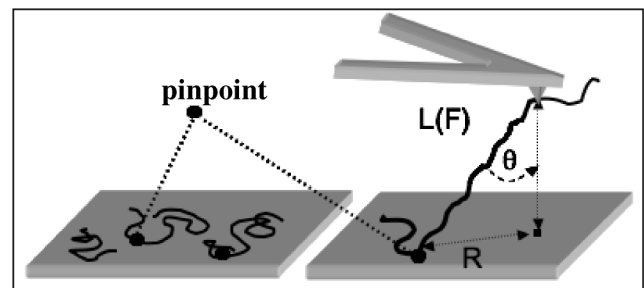
FIG. 1. Schematics of the experimental strategy. Polymers were covalently pinned onto a surface at very low density, restricting only their overall diffusion, not their segment mobility. Individual polymers were randomly picked up with an AFM-cantilever tip and stretched.

into an adsorption enthalpy of $\approx 2k_B T/\text{nm}$ or little more than $k_B T$ for a polymer segment on the order of the Kuhn length. According to different references [2,30], the polymer is expected to be thus largely restricted to the surface.

We now lowered an AFM tip to the surface and picked such a pinned polymer. We then stretched it upon retracting the tip from the surface (see Fig. 1). Many studies have shown that polymers may be attached to the tip of an AFM cantilever if the contact force is increased above a certain threshold [10,31]. Since the pickup of the pinned polymer at the surface is random, we define with this process an arbitrary section of the polymer between the pinning point and the pickup point. The distance between these two points on the surface and the contour length of this polymer section obey the same scaling law as the end-to-end distance and the contour length of the entire polymer. In particular, the scaling exponent ν, which determines the degree of swelling of the polymer, will be the same in both cases, provided the section is much longer than the Kuhn length b.

The task is thus to measure the two lengths L_c and $\langle |R| \rangle$—the end-to-end distance, which the polymer had at the moment of the pickup—by retracting the tip from the surface in a suitable manner. Figure 1 highlights the geometry. Obviously, the polymer section is stretched at an angle θ when the AFM tip is retracted normal to the surface, and the end-to-end distance is simply the projection of the stretched polymer onto the surface. An appropriate strategy would be to determine the position of the pinpoint relative to the tip position. In principle, this could be achieved by scanning the tip at constant force. The tip would then move on a hemisphere with the pinpoint as the center. To avoid permanent high load on the polymer, we chose a scheme where the tip is scanned at constant height. Nevertheless, also here a basic difficulty arises from the fact that the cantilever geometry breaks the symmetry of the experiment. The horizontal components of the force, which act on the tip upon stretching a polymer, exert a torque on the tip. This results in an additional bend of the cantilever, which leads to a cross talk of the lateral forces into the measured normal force. This effect needs first to be evaluated in order to be able to correct for the asymmetric bending effects of the cantilever.

To analyze this problem, the force acting on the cantilever was measured for different pulling geometries. Figure 2(a) shows the force extension relation measured for a single CMA polymer, which was picked up following the procedure given above. The hump reflects the force-induced lengthening of the pyranose rings from their ground state chair conformation ($^4C_1$) to the boat conformation [10,32,33]. In the following, we use this transition as an internal sensor for the force acting along the polymer backbone. The dashed line gives the best fit of the force extension relation based on the freely jointed chain model with enthalpic segment elasticity. The two conformations of the segments are modeled by a two-level system according to the following equation with $N_{\text{ground}}/N_{\text{boat}} = \exp(\Delta G/k_B T)$ [13,34]:
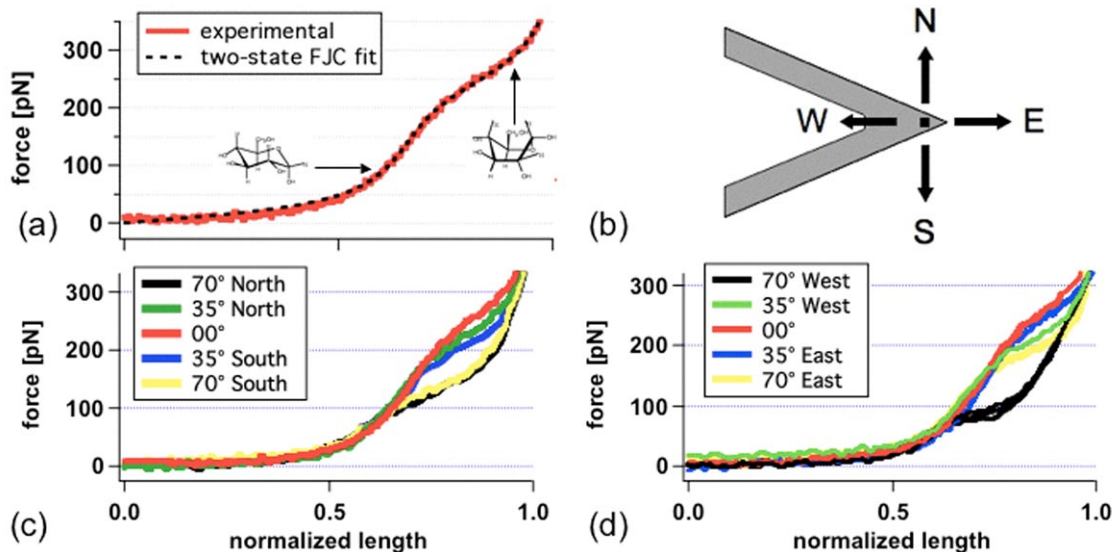
FIG. 2 (color online).   Force extension curve (a) for a long CMA polymer, with the two-state FJC fit (dashed black line). Between 200 and 300 pN, the pyranose rings change their conformation, which was used as an internal force sensor in the polymer. In (b), the geometry of the cantilever is sketched. Normal forces acting on the cantilever tip result in an out-of-plane bend of the cantilever along the east-west direction. This bend is measured with the reflected laser beam and after calibration converted into a force. Tangential forces acting on the tip result in a torque and cause an additional bend of the cantilever. However, only the east-west components of the lateral forces are picked up this way. The north-south components are not detected. This effect can be seen in (c) and (d), where this bend is measured when pulled at an angle with respect to the surface. Whereas in the north-south direction (c) the transition force decreases with the angle, the force additionally differs markedly, when pulled east or west (d).

$$L(F) = N_S\left(\frac{L_{\text{ground}}}{e^{-\Delta G/k_B T} + 1} + \frac{L_{\text{boat}}}{e^{+\Delta G/k_B T} + 1}\right)$$
$$\times\left[\coth\left(\frac{FL_K}{k_B T}\right) - \frac{k_B T}{FL_K}\right] + N_S\frac{F}{K_s},$$

where N_s is the total number of segments, L_{ground} and L_{boat} are the length of the conformation of the stress-free and under-stress pyranose rings, respectively. L_K is the Kuhn length (we use a different symbol for the Kuhn length as before to distinguish that they were derived differently), K_S the segment elasticity, and ΔG the free energy difference. For the CMA fit in Fig. 2(a), we used values from the literature: $L_{\text{ground}} = 0.45$ nm, $L_{\text{boat}} = 0.54$ nm, $L_K = 0.45$ nm, $K_C = 28$ N/m, and $\Delta G = 6k_B T$ [35]. The only free parameter is the contour length ($L_c = L_K N_S$) of the polymer, which is extracted from the fit with an accuracy of better than 1 nm [note: since $\langle\sin(\theta)\rangle$ scales with N^{g-1}, particularly long polymers were chosen to reduce the cross talk of lateral forces]. As a control, we varied the Kuhn length in the fitting procedure and found the literature value to provide the best fit also for our curves. In Fig. 2(b), a polymer was picked up and stretched obliquely by retracting the tip at different angles towards the normal and in different directions relative to the cantilever geometry [cantilever C from MLCT-AUHW; Veeco Instruments GmbH, Mannheim, Germany. Deviations (for the west and east directions) occur at all cantilevers, because of the lateral asymmetry of the cantilever.]. As can easily be seen in Figs. 2(c) and 2(d), the conformation transition of the polymer occurs at different normal forces for different angles. Whether the tip was moved north or south had a negligible effect, as was to be expected.

The normal force acting on the cantilever decreases with the factor of $\cos(\theta)$. Figure 2(d) shows the same kind of experiment. However, here the difference in torque between east and west alters markedly the force at which the transitions occur. The torque increases (west) or reduces (east) the deflection of the cantilever caused by the normal component of the backbone force. To summarize, at the same backbone force, the measured deflection signal of the AFM cantilever depends on angle and direction. For a precise measurement of the polymer pinpoint, this needs to be taken into account.

From the interpolation between many such curves [36] as shown in Figs. 2(c) and 2(d), a force map was created (Fig. 3), which gives the normal component of the force acting on the sugar polymer that is pinned at the origin when the tip is scanned parallel to the surface at a certain height. The asymmetry of the cantilever results in marked distortion, which is best notable at the hump ring of the boat-chair transition. It should be pointed out here that a shift of the pinpoint of the polymer results in a shift of the force map relative to the zero position of the cantilever tip. This means that this force map can now be used as a master surface to analyze the force map measured on an arbitrary pinned polymer such as the one shown in Fig. 4. In this
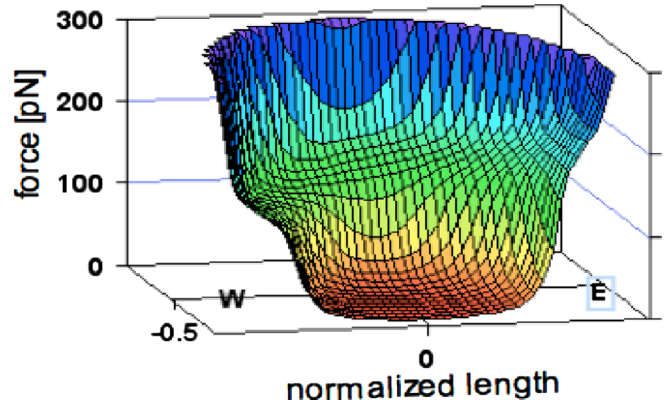
FIG. 3 (color online). Master-force map of a CMA molecule generated by interpolation between many force curves such as the ones in Fig. 2. It gives the normal force component when the tip is scanned above the surface at a constant height of $1/3$ of its total length. The asymmetry of the force map reflects the cantilever asymmetry as described before.

experiment, the tip was moved along the trace depicted in Fig. 4(a). After the polymer was picked up, the tip was lifted normal and then scanned parallel to the surface in squares with increasing diameter. (By this approach, the polymer is pulled from 2D in 3D conformation. However, the anchor point of the polymer at one end, which is
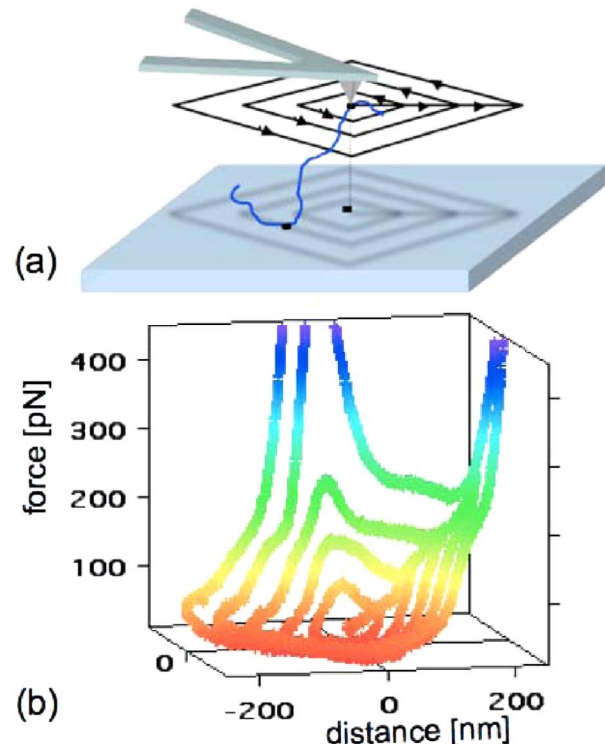
FIG. 4 (color online). In (a), the protocol for the cantilever motion is sketched. The cantilever is retraced and scanned parallel to the surface while the force is recorded. (b) The resulting force curve. Obviously, only a segment of the entire force map was visited. In comparison with the master curve, the pinpoint was localized southwest of the origin (see Fig. 3).
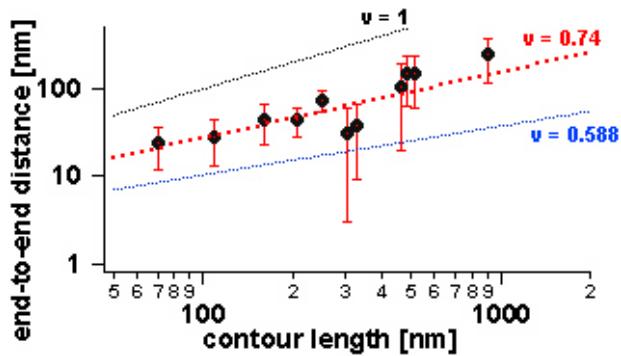
FIG. 5 (color online). End-to-end distance of CMA-polymer sections plotted against their contour length. The red dashed line is the fit with a scaling factor of 0.74 ± 0.04 and a segment length of $b = 0.44 \pm 0.14$ nm. The blue and black dotted lines are plots with $\nu = 0.588$ and $\nu = 1$ with $b = 0.44$ nm, respectively.

determined by this step, is unaltered.) The measured normal force is shown in Fig. 4(b). As can be seen, the force map is quite asymmetric. This is because the pinpoint of the polymer is located southwest of the tip origin and so only roughly a quarter segment of the ''bowl'' was visited.

A set of polymers was investigated following the procedure given above; the distance between pinpoint and pickup point and as such the end-to-end distance of the polymer section were determined [37] by fitting the traces to the master-force map. (All data analysis was done by self-written procedures in IGOR 5.03.) Also determined was the contour length by fitting the extension traces of the polymer vertical to the surface.

In Fig. 5, the end-to-end distances (binned with ± 10 nm) of 97 CMA-polymer sections were plotted double logarithmically against their contour lengths. From the slope, the scaling factor ν was determined to be 0.74 ± 0.04, which is close to the expected value for a 2D polymer (0.75). This signifies that the polymer rearranges on the surface after adsorption [38] and is highly dynamic [39].

If one would assume equality and not only proportionality in the scaling law for the end-to-end distance, the y intercept in Fig. 5 would provide the Kuhn length with a value of $b = 0.44 \pm 0.14$ nm, which is in very good agreement with the Kuhn length L_K derived from the freely jointed chain (FJC) fits and the chemical structure for a single pyranose ring [40].

We envision that this approach to measure conformational parameters of dynamic polymers *in situ* is applicable to a broad spectrum of adsorbed, tethered, pinned, or grafted polymers. As a side effect, this study here has also shed light on the question of whether tangential contributions to the normal force in single molecule force spectroscopy experiments need to be considered.

[1] P. G. de Gennes, *Scaling Concepts in Polymer Physics* (Cornell University, Ithaca, 1979).
[2] R. H. C. Michael Rubinstein, *Polymer Physics* (Oxford University Press, New York, 2003).
[3] C. Holm *et al.*, in *Polyelectrolytes with Defined Molecular Architecture II*, Advances in Polymer Science Vol. 166 (Springer, New York, 2004), pp. 67-111.
[4] O. V. Borisov *et al.*, Eur. Phys. J. E **6**, 37 (2001).
[5] A. Milchev and K. Binder, Macromolecules **29**, 343 (1996).
[6] E. Eisenriegler, K. Kremer, and K. Binder, J. Chem. Phys. **77**, 6296 (1982).
[7] B. Maier and J. O. Radler, Phys. Rev. Lett. **82**, 1911 (1999).
[8] J. P. C. M. Daoud, B. Farnoux, G. Jannink, G. Sarma, H. Benoit, C. Duplessix, C. Picot, and P. G. de Gennes, Macromolecules **8**, 804 (1975).
[9] Y. E. Y. Miyaki and H. Fujita, Macromolecules **11**, 1180 (1978).
[10] M. Rief *et al.*, Science **275**, 1295 (1997).
[11] M. Rief *et al.*, Science **276**, 1109 (1997).
[12] S. Cui *et al.*, J. Am. Chem. Soc. **128**, 6636 (2006).
[13] F. Oesterhelt, M. Rief, and H. E. Gaub, New J. Phys. **1**, 6 (1999).
[14] T. Hugel *et al.*, Phys. Rev. Lett. **94**, 048301 (2005).
[15] J. Kas *et al.*, Europhys. Lett. **21**, 865 (1993).
[16] C. M. Schroeder *et al.*, Phys. Rev. Lett. **95**, 018301 (2005).
[17] C. Anselmi, P. DeSantis, and A. Scipioni, Biophys. Chem. **113**, 209 (2005).
[18] F. Valle *et al.*, Phys. Rev. Lett. **95**, 158105 (2005).
[19] H. G. Hansma *et al.*, Nucleic Acids Res. **21**, 505 (1993).
[20] L. Bourdieu, P. Silberzan, and D. Chatenay, Phys. Rev. Lett. **67**, 2029 (1991).
[21] J. Marek *et al.*, Cytometry **63A**, 87 (2005).
[22] N. Severin *et al.*, Nano Lett. **6**, 1018 (2006).
[23] F. Kühner, M. Erdmann, and H. E. Gaub, Langmuir (in press).
[24] T. Hugel *et al.*, Macromolecules **34**, 1039 (2001).
[25] M. Seitz *et al.*, Chem. Phys. Chem. **4**, 986 (2003).
[26] X. Chatellier *et al.*, Europhys. Lett. **41**, 303 (1998).
[27] Aminoslide_A, Schott, Nexterion, Mainz, Germany.
[28] F. Kühner *et al.*, Biophys. J. **87**, 2683 (2004).
[29] See EPAPS Document No. E-PRLTAO-97-010647 for regular force curves desorbing CMA of the amino surface and imaging in tapping mode after critical point drying. For more information on EPAPS, see http://www.aip.org/pubservs/epaps.html.
[30] P. G. de Gennes, J. Phys. (Paris) **37**, 1445 (1976).
[31] M. Rief, H. Clausen-Schaumann, and H. E. Gaub, Nat. Struct. Biol. **6**, 346 (1999).
[32] P. E. Marszalek, H. Li, and J. M. Fernandez, Nat. Biotechnol. **19**, 258 (2001).
[33] P. E. Marszalek *et al.*, Nature (London) **396**, 661 (1998).
[34] M. Rief, J. M. Fernandez, and H. E. Gaub, Phys. Rev. Lett. **81**, 4764 (1998).
[35] H. Li *et al.*, Chem. Phys. Lett. **305**, 197 (1999).
[36] F. Kühner and H. Gaub, Polymer **47**, 2555 (2006).
[37] J. Wilhelm and E. Frey, Phys. Rev. Lett. **77**, 2581 (1996).
[38] C. Rivetti, M. Guthold, and C. Bustamante, J. Mol. Biol. **264**, 919 (1996).
[39] S. Manneville *et al.*, Europhys. Lett. **36**, 413 (1996).
[40] P. E. Marszalek *et al.*, Nature (London) **396**, 661 (1998).